

# Measurement of the Intracrystalline Self-Diffusion of Xenon in Zeolites by the NMR Pulsed Field Gradient Technique

Wilfried Heink, Jörg Kärger,\* Harry Pfeifer, and Frank Stallmach

Contribution from the Sektion Physik der Karl-Marx-Universität Leipzig, Linnēstrasse 5, DDR-7010 Leipzig, German Democratic Republic. Received July 6, 1989

**Abstract:** With use of  $^{129}\text{Xe}$  NMR, the NMR pulsed field gradient technique is applied to study the self-diffusion of xenon adsorbed on zeolites NaX, NaCaA, and ZSM-5. In their dependence on both the type of adsorbent and the sorbate concentration, the self-diffusion coefficients are found to follow the same patterns as previously determined for methane by  $^1\text{H}$  NMR. For NaCaA, the comparison of the present results with literature data reveals large discrepancies, while recent computer simulations of xenon self-diffusion in ZSM-5 are found to be in reasonable agreement.

In the last few years, xenon has turned out to be an efficient adsorbate for probing the pore structure and the internal surface of adsorbents by means of NMR spectroscopy.<sup>1-3</sup> The advantage of xenon in comparison to other adsorbates is brought about by the large chemical shifts of  $^{129}\text{Xe}$  NMR as a consequence of the large electron shell, and by the fact that xenon as a noble gas leaves the adsorbent structure essentially unaffected. In particular, in zeolite research  $^{129}\text{Xe}$  NMR has been successfully applied for probing pore and channel dimensions,<sup>4</sup> cation distributions,<sup>5</sup> reaction sites,<sup>6</sup> and structural peculiarities.<sup>7</sup> Following the pioneering work of Fraissard and co-workers, it is now applied as a routine method in various laboratories.<sup>8-10</sup>

The advent of  $^{129}\text{Xe}$  NMR in zeolite research has been accompanied by some controversy in the interpretation of the obtained spectra. In particular, on observing different, distinct lines in the NMR spectra and attributing them to certain states or regions of the xenon atoms within the adsorbate-adsorbent systems, one has to imply that the rate of exchange between these states or regions is less than the difference in the Larmor frequencies of these lines.<sup>11</sup> If the spatial separation of the respective regions is known, an estimate of the diffusivities of the xenon atoms within the sample becomes possible.<sup>12</sup> It is obvious that in such cases the validity of the interpretation of the  $^{129}\text{Xe}$  NMR spectra would be substantially supported if the diffusivities could be measured directly. In principle, such a possibility is provided by the NMR pulsed field gradient technique.<sup>13,14</sup> As yet, however, in zeolite research due to the poorer measuring conditions for all other nuclei, NMR self-diffusion measurements have nearly exclusively been carried out with molecules containing hydrogen.<sup>15,16</sup> It is only due to the substantial improvement of the experimental

conditions in the last few years that  $^{129}\text{Xe}$  NMR self-diffusion measurements have become possible. To our knowledge, in the following the first coefficients of intracrystalline self-diffusion of xenon in zeolites determined by the NMR pulsed field gradient technique will be presented.

## Theoretical Section

The NMR pulsed field gradient technique is based on the application of the radio frequency pulse sequences for generating the primary or the stimulated echo,<sup>13,14</sup> where during two time intervals of duration  $\delta$  the constant magnetic field is superimposed by two inhomogeneous magnetic fields with the field gradient  $g$ . Under the influence of these "field gradient pulses", the magnitude of the NMR signal (the "spin-echo intensity") is reduced by the factor<sup>13,14</sup>

$$\Psi(\delta g, \Delta) = \exp\{-\gamma^2 \delta^2 g^2 D \Delta\} \quad (1)$$

with  $\Delta$  denoting the separation between the two (identical) field gradient pulses, which for simplicity have been assumed to be much larger than the pulse width  $\delta$ .  $\gamma$  stands for the gyromagnetic ratio of the nuclei under consideration, and  $D$  denotes the self-diffusion coefficient. In a homogeneous medium, the self-diffusion coefficient is related to the mean-square displacement of the diffusing particles during the observation time  $t$  by Einstein's relation

$$\langle r^2(t) \rangle = 6Dt \quad (2)$$

Inserting this expression into eq 1 yields

$$\Psi(\delta g, \Delta) = \exp\{-\gamma^2 \delta^2 g^2 \langle r^2(\Delta) \rangle / 6\} \quad (3)$$

It appears from eq 3 that the NMR pulsed field gradient technique is directly sensitive to the mean-square displacement of the observed particles over an observation time determined by the separation of the field gradient pulses. According to eq 3 the mean-square displacement may be determined from the slope of the semilogarithmic representation of the spin-echo intensity versus the squared gradient width,  $\delta^2$ . Equation 2 indicates that there should be a linear relation between the mean-square displacement and the observation time as long as the diffusion phenomena observed are within a homogeneous region. On observing the adsorbate diffusion in zeolites this linearity can be used, therefore, to check whether the diffusivities observed are in fact within the intracrystalline space. In this case, the slope of the  $\langle r^2(\Delta) \rangle$  vs  $\Delta$  plot directly yields the coefficient of intracrystalline self-diffusion. Any deviation from linearity has to be attributed to additional effects such as the influence of diffusional barriers at the outer surfaces of the crystals or of intercrystalline mass transfer<sup>15,16</sup> or, at least theoretically, to deviations from Einstein's relation (eq 2).<sup>17,18</sup>

(1) Ito, T.; Fraissard, J. In *Proceedings of the 5th International Conference on Zeolites*, Naples, 1980; p 510.

(2) Ripmeester, J. J. *Am. Chem. Soc.* **1982**, *104*, 289.

(3) Fraissard, J.; Ito, T. *Zeolites* **1988**, *8*, 350-361.

(4) Demarquay, J.; Fraissard, J. *J. Chem. Phys. Lett.* **1987**, *136* (3,4), 314.

(5) Ito, T.; Fraissard, J. *J. Chem. Soc., Faraday Trans. I* **1987**, *83*, 451.

(6) Fraissard, J.; Ito, T.; de Menorval, L. C. In *Proceedings of the 8th International Congress on Catalysis 111-25*, Berlin, 1984.

(7) Ito, T.; de Menorval, L. C.; Guerrier, E.; Fraissard, J. *Chem. Phys. Lett.* **1984**, *111*, 3271.

(8) Scharpf, E. W.; Grecely, R. W.; Gates, B. C.; Dybowski, C. *J. Phys. Chem.* **1987**, *90*, 9.

(9) Shoemaker, R.; Apple, T. *J. Phys. Chem.* **1987**, *91*, 4024.

(10) Chmelka, B. F.; Ryoo, R.; Liu, S.-B.; de Menorval, L. C. *J. Am. Chem. Soc.* **1988**, *110*, 4465.

(11) Winkler, H.; Michel, D. *Adv. Colloid Interface Sci.* **1985**, *23*, 149.

(12) Kärger, J.; Pfeifer, H.; Fraissard, J. *Z. Phys. Chem. (Leipzig)* **1987**, *268*, 195.

(13) Stejskal, E. D.; Tanner, J. E. *J. Chem. Phys.* **1965**, *42*, 288.

(14) Kärger, J.; Pfeifer, H.; Heink, W. *Adv. Magn. Reson.* **1988**, *12*, 1.

(15) Kärger, J.; Pfeifer, H. *Perspectives in Molecular Sieve Science*; Flank, W. H., Whyte, T. E., Eds.; ACS Symp. Ser. No. 268; American Chemical Society: Washington, DC, 1988; p 377.

(16) Kärger, J.; Pfeifer, H. *Zeolites* **1987**, *7*, 90.

(17) Harder, H.; Havlin, S.; Bunde, A. *Phys. Rev. B* **1987**, *36*, 3874.

(18) Kärger, J.; Pfeifer, H.; Vojta, G. *Phys. Rev. A* **1988**, *37*, 4514.

### Experimental Section

The signal-to-noise ratio in NMR spectroscopy is proportional to  $c\gamma^{5/2}$ , with  $c$  and  $\gamma$  denoting respectively the concentration of the resonating nuclei and their gyromagnetic ratio.<sup>19</sup> With respect to both these quantities,  $^1\text{H}$  NMR provides by far the best conditions. Thus, e.g., for  $^{129}\text{Xe}$   $\gamma$  is equal to  $0.74 \times 10^8 \text{ T}^{-1} \text{ s}^{-1}$ , in comparison to  $\gamma_{^1\text{H}} = 2.67 \times 10^8 \text{ T}^{-1} \text{ s}^{-1}$  for protons. The realization of sufficiently high values of  $c$  in proton NMR is facilitated by the large natural abundance of the NMR active hydrogen isotope  $^1\text{H}$  (99.985%, in comparison to 26.24%  $^{129}\text{Xe}$  in natural xenon). In addition, on applying conveniently selected adsorbate molecules, the amount of hydrogen atoms per unit volume of the adsorbent may be chosen to be higher than for any other atom. This is in particular true for xenon, whose volume is even slightly larger than that of methane (the gas-kinetic diameters are 0.49 and 0.41 nm, respectively<sup>20</sup>), which comprises no less than four hydrogen atoms.

In principle, the effect of low signal-to-noise ratios may be compensated by a sufficiently large number of signal accumulations. In NMR pulsed field gradient spectroscopy this procedure is complicated by the fact that the detection of small radio frequency signals necessitates the application of phase-sensitive detection, which in turn requires a relative stability of the constant magnetic field of about  $10^{-7}$  during the measurement.<sup>14</sup> In conventional iron magnets, however, the necessary flux stabilization is most likely to be set out of the control range under the influence of pulsed field gradients of large intensity and with short rise and fall times, as to be required, in general, for self-diffusion measurement in zeolites. By the use of a large-gap iron magnet this difficulty could be circumvented. The width and diameter of the gap were 50 and 500 mm, respectively. It turned out that in such an arrangement, with the gradient coil ("quadrupole coil")<sup>14</sup> in the center of the gap and the flux coils at the edge of the pole faces, the flux stabilization also remained in the control range during the gradient pulses. In this way, accumulation numbers of typically 1000 could be realized.

The NMR self-diffusion measurements have been carried out by means of a home-built spectrometer (UDRIS) at a resonance frequency of 24.9 MHz corresponding to magnetic field intensities of 2.1 T for  $^{129}\text{Xe}$  and of 0.6 T for  $^1\text{H}$ . The pulsed field gradient intensities could be varied up to a value of  $g = 4 \text{ T/m}$  with a maximum duration of  $\delta = 1.2 \text{ ms}$ .<sup>14</sup> In all cases the measuring temperature was 293 K.

A most essential supposition of the NMR pulsed field gradient technique is the identity of the two gradient pulses. Any difference in the "area"  $\delta g$  of the two gradient pulses leads to an echo attenuation that might be erroneously interpreted as brought about by diffusion. In general, this source of error is excluded by varying the width of one of the two gradient pulses until the signal maximum is obtained. In the present study, we have carried out this procedure for any of the applied sets of gradient intensities and pulse widths and separations by  $^1\text{H}$  NMR, since in this case the NMR signal is directly visible without any accumulation. The adjustment was facilitated by applying a sample of vacuum grease, whose diffusivity turned out to be so small that after the correct choice of the gradient widths there was no echo attenuation at all. The thus adjusted gradient widths have been applied in all subsequent measurements. A repetition of the adjustment procedure showed that the chosen values remained correct over the whole measuring period. The absolute value of the mean square displacement of xenon was obtained by comparing the slope of the  $\ln \Psi$  vs  $\delta^2$  representation as observed by  $^{129}\text{Xe}$  NMR with that of water, determined by  $^1\text{H}$  NMR with the same field gradient program. At 239 K the self-diffusion coefficient of water is  $(2.04 \pm 0.08) \times 10^{-9} \text{ m}^2 \text{ s}^{-1}$ .<sup>2</sup> Via eq 2 it may be easily transferred into the mean-square displacement during the given observation time  $\Delta$ .

It appears from eq 3 that for identical field gradient programs and mean-square displacements the slopes of the  $\ln \Psi$  vs  $\delta^2$  representations are proportional to the squares of the gyromagnetic ratios. With the above data one finds  $\gamma_{^1\text{H}}^2/\gamma_{^{129}\text{Xe}}^2 \approx 13$ , so that for identical mobilities the slope of the  $\ln \Psi$  vs  $\delta^2$  representation for  $^{129}\text{Xe}$  is by a factor of 13 smaller than that for  $^1\text{H}$ . This fact leads to a further limitation of self-diffusion measurements by  $^{129}\text{Xe}$  NMR. In order to effect the same reduction of the signal intensity as in  $^1\text{H}$  NMR, the mean-square displacements must be larger by a factor of 13. If one is interested in the observation of intracrystalline self-diffusion, this necessitates the application of sufficiently large zeolite crystallites.

In our experiments, we have used zeolites of type A and X with mean crystallite diameters of 20 and 50  $\mu\text{m}$  and of silicalite (ZSM-5 with a ratio  $\text{Si}/\text{Al} \geq 10^3$ ) with crystal dimensions of  $100 \times 30 \times 30 \mu\text{m}^3$ , which

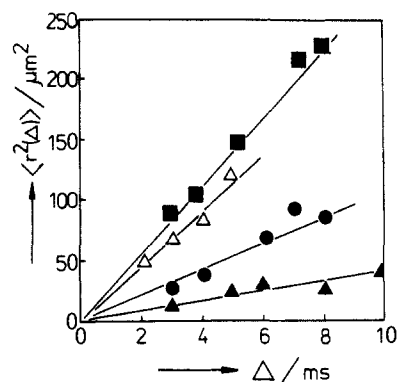


**Figure 1.** Mean-square displacement of the xenon atoms in zeolites NaX (■), Na 63% CaA (●), and ZSM-5 (silicalite, ▲) in dependence on the observation time and, for comparison, of methane in silicalite (Δ). The sorbate concentration is in all cases about 3 atoms (molecules) per 24 Si (Al) atoms.

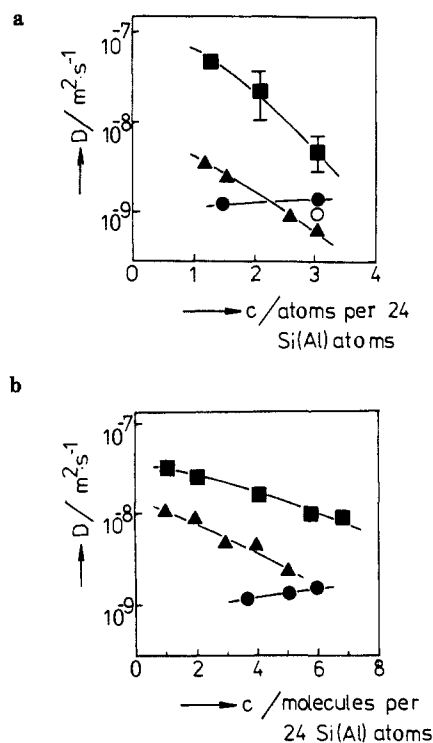


**Figure 2.** Concentration dependence of the intracrystalline self-diffusion coefficient of xenon (a) and methane (b, from ref 26) in zeolites NaX (■) Na 63% CaA (●), Na 45% CaA (○), and ZSM-5 (▲).

have been provided by Zhdanov and Feokistova, Academy of Sciences of the USSR, Leningrad.<sup>22,23</sup> They turned out to be large enough to guarantee the measurement of intracrystalline self-diffusion over a sufficiently large range of observation times. The NaCa type zeolites have been obtained from the NaA form by cation exchange from a solution of  $\text{CaCl}_2$ .<sup>24</sup> The NMR self-diffusion measurements have been carried out with the loaded zeolites contained in sealed glass sample tubes with an outer diameter of 10 mm and a filling height of about 20 mm. For sample preparation, the zeolite material has been spread as a thin layer with a depth of less than 3 mm and heated under continuous evacuation with a heating rate of 10 deg/h until a final temperature of 673 K and a final pressure of less than 0.1 Pa is reached ("shallow bed" activation<sup>15</sup>). Xenon has been introduced into the thus activated sample by freezing at the temperature of liquid nitrogen from a well-defined volume at room

(19) Abragam *Principles of Nuclear Magnetism*; Oxford University Press: New York, 1961.

(20) Landolt-Börnstein *Zahlenwerke und Funktionen*; Springer-Verlag: Berlin, 1950; Band I, Teil I, S. 325/370.

(21) Weingärtner, *Z. Phys. Chem. (N.F.)* **1982**, *132*, 129.

(22) Zhdanov, S. P.; Kvoshchov, S. S.; Samulevich, N. N. *Synthetic Zeolites*; Khimia: Moscow, 1981.

(23) Feokistova, N. N.; Zhdanov, S. P.; Lutz, W.; Bülow, M. *Zeolites* **1989**, 136.

(24) Wolf, F.; Danes, F.; Pilchowski, K. *Z. Phys. Chem. (Leipzig)* **1973**, *252*, 33.

(25) Kerr, G. *Inorg. Chem.* **1955**, *5*, 1539.

temperature. The achieved loadings were checked gravimetrically as well as by comparing the intensities of the NMR signals (free induction decays).

## Results

Figure 1 provides an example of the measurement of the mean-square displacements of the xenon atoms in the three different zeolite types NaX, NaCaA, and ZSM-5 in dependence on the observation time. For comparison, the data for methane in ZSM-5 are also included. According to eq 2, each of the observed linear relations yields a value for the self-diffusion coefficient. Figure 2a shows the results of all  $^{129}\text{Xe}$  measurements in a representation of the thus determined self-diffusion coefficients in dependence on the sorbate concentrations. The sorbate concentrations are given in atoms per 24 Si(Al) atoms, corresponding to one channel intersection in the case of ZSM-5 and to one large cavity in the case of the X and A type zeolites. The error bars indicate the uncertainty in the self-diffusion coefficients resulting from the scattering of the experimental data of the mean-square displacement with respect to the linear dependence on the observation time.

For comparison, Figure 2b represents the results of previous methane self-diffusion measurements in the same zeolites.<sup>26</sup>

In addition to the data obtained with the NaCaA zeolite with 63% of the sodium cations exchanged by calcium ( $\text{Na}_{4.4}\text{Ca}_{3.8}\text{A}$ ), Figure 2a also contains the result of a comparative experiment with a NaCaA zeolite at a lower cation exchange (45%:  $\text{Na}_{6.6}\text{Ca}_{2.7}\text{A}$ ).

## Discussion

On starting self-diffusion measurements with a new system, it is essential to provide additional support of the validity of the obtained values. One of the most convenient procedures used for this purpose in the past was the measurement of the temperature dependence of the self-diffusion coefficient.<sup>27,28</sup> In an Arrhenius plot, the measured self-diffusion coefficient will yield a linear dependence as long as the observed displacements are within the individual crystallites. As soon as the displacements become comparable with the diameters of the crystallites, the Arrhenius plots show noticeable deviations from linearity. Depending on the magnitude of possible transport resistances on the crystal surface and the mobility in the intercrystalline space, these deviations may tend to higher or lower values. Remaining in the linear region of the Arrhenius plot, one may be sure, therefore, to measure intracrystalline diffusivities.

Since with the present probe head of the NMR spectrometer we were only able to measure at room temperature, we have modified this procedure by measuring the molecular mean-square displacements at a fixed temperature for different observation times. As demonstrated in Figure 1, over a fairly large range of observation times a linear dependence has been observed. Corresponding to this finding, also for the largest observation times indicated in Figure 1, the determined root-mean-square displacements turned out to be much smaller than the crystallite diameters. This is just the behavior required for intracrystalline self-diffusion. Clearly, this procedure is also applicable to "conventional"  $^1\text{H}$  NMR self-diffusion measurements as indicated with the data for methane in ZSM-5, included in Figure 1.

In addition, the observed linearity of the relation between the mean-square displacement and the observation time indicated that adsorbate propagation in zeolites obeys the laws of ordinary diffusion to be expected for such regular adsorbent frameworks.

The representation of the diffusivities of xenon and of methane in Figure 2, a and b, shows similar tendencies: For both adsorbates, the mobility in zeolite NaX is found to be higher than that in the other adsorbents. This corresponds to the fact that the diameters of the windows between the large cavities in the X-type structure (0.75 nm) are considerably larger than the corresponding

**Table I.** Comparison of the Determined Self-Diffusion Coefficients for Xenon in Zeolite NaCaA with Literature Data

	computer simulation ref 35	uptake measurements		
		ref 34	ref 33	present work
<i>T</i> , K	303	303	323	293
<i>C</i> , atoms per cavity	1	1	1	$1.5 \pm 0.3$
<i>D</i> , $\text{m}^2 \text{s}^{-1}$	$3.3 \times 10^{-12}$	$1.2 \times 10^{-11}$	$1 \times 10^{-14}$	$1.5 \times 10^{-9} \pm 30\%$

**Table II.** Comparison of the Determined Self-Diffusion Coefficients for Xenon in ZSM-5 with the Results of a Computer Simulation<sup>36</sup>

<i>C</i> , atoms per channel intersection	<i>D</i> , $\text{m}^2 \text{s}^{-1}$ computer simulation <sup>36</sup>	present work
1	$1.86 \times 10^{-9}$	$4 \times 10^{-9}$
2		$3 \times 10^{-9}$
3	$0.87 \times 10^{-9}$	$0.8 \times 10^{-9}$
4	$0.37 \times 10^{-9}$	

diameters in zeolite NaCaA (0.4–0.5 nm) or the channel diameters in zeolite ZSM-5 (0.55 nm).

In zeolite A, the degree of calcium exchange determines the relative number of "open" windows, i.e. the number of windows unblocked by cations, which thus are easily penetrable for the adsorbate molecules.<sup>29,30</sup> A numeric calculation given in ref 29 yields that a reduction of the calcium content from 63% to 45% should reduce the diffusivity by a factor of about 2. The experimental data shown in Figure 2a at a sorbate concentration of 3 xenon atoms per cavity are in satisfactory agreement with this prediction, which, in turn, may be taken as an indication that the calcium cations are in fact homogeneously distributed over the crystallites.

Considering the concentration dependence of the diffusivities, for xenon and methane again the same tendencies are observed: While in zeolite NaX and ZSM-5 the diffusivities are found to decrease monotonously with increasing concentration, for zeolite NaCaA the diffusivities either remain constant or slightly increase with increasing concentration. It has been demonstrated in ref 31 that concentration dependences of the first type are due to a reduction of the jump length (in NaX) or of the jump rate (in ZSM-5), while the latter behavior results if mass transfer is controlled by the passage through an "activated" state as represented by the windows in the A type structure. Obviously, the similar size and shape of xenon and methane lead to coinciding dependences.

In the last few years, the diffusivity of xenon in zeolite has been investigated by both uptake measurements<sup>32</sup> and computer simulation. Table I gives a comparison of literature data for the system xenon/NaCaA at a calcium exchange of about 63% with the corresponding value of the present study. In analogy to similar comparisons for other systems (cf., e.g. refs 27 and 32) the NMR data appear to be much larger than the results of the uptake experiments. In many cases this discrepancy has been found to be caused by the influence of the finite rate of adsorption heat dissipation which, if not taken into account, leads to completely wrong diffusion data from uptake experiments.<sup>32</sup>

(29) Ruthven, D. M. *Can. J. Chem.* **1974**, *52*, 3523.

(30) Caro, J.; Kärger, J.; Finger, G.; Pfeifer, H.; Schöllner, R. *Z. Phys. Chem. (Leipzig)* **1976**, *257*, 903.

(31) Pfeifer, H.; Kärger, J.; Germanus, A.; Schirmer, W.; Bülow, M.; Caro, J. *Adv. Sci. Technol.* **1985**, *2*, 229.

(32) Ruthven, D. M. *Principles of Adsorption and Adsorption Processes*; John Wiley: New York, 1984.

(33) Ruthven, D. M.; Derrah, R. J. *J. Chem. Soc., Faraday Trans. 1* **1975**, *71*, 2031.

(34) Dubinin, M. M.; Gorlov, V. A.; Voloshchuk, A. M. *Proc. Internat. Conf. Zeolites, Naples*; Rees, L. V. C., Ed.; Heyden: London, 1980.

(35) Bakaev, V. A.; Smirnova, L. F. *Izv. Akad. Nauk SSSR Ser. Khim.* **1978**, 284.

(36) Pickett, S. D.; Nowak, A. K.; Peterson, B. K.; Swift, J.; Cheetham, A. K.; den Ouden, C. J. J.; Smit, B.; Post, M. F. M. *J. Phys. Chem.*, submitted for publication.

(26) Caro, J.; Bülow, M.; Schirmer, W.; Kärger, J.; Heink, W.; Pfeifer, H. *J. Chem. Soc., Faraday Trans. 1* **1985**, *81*, 2543.

(27) Kärger, J.; Caro, J. *J. Chem. Soc., Faraday Trans. 1* **1977**, *73*, 1363.

(28) Caro, J.; Hočevár, S.; Kärger, J.; Riekert, L. *Zeolites* **1986**, *6*, 213.

Table II shows the results of recent computer simulations for the xenon self-diffusion in ZSM-5. It is remarkable that both the absolute values and the predicted concentration dependence are in reasonable agreement with the NMR data.

### Conclusion

$^{129}\text{Xe}$  NMR has been successfully applied to study the self-diffusion of xenon in zeolites. The measurement of the mean-square displacement in dependence on the observation time yielded a linear relation as required for ordinary, intracrystalline self-diffusion. In zeolites NaX and ZSM-5, the self-diffusion coefficients were found to decrease with increasing concentration while

for zeolite NaCaA they are essentially constant. The highest diffusivities were observed in zeolite NaX. This is in agreement with the fact that due to the internal pore structure the steric restrictions of molecular propagation in zeolite NaX are smaller than those in NaCaA and ZSM-5.

For zeolite NaCaA the obtained diffusivities are by several orders of magnitude larger than literature data based on both uptake experiments and computer simulation. Recent computer simulations of xenon diffusion in ZSM-5, however, are found to be in satisfactory agreement.

Registry No. Xe, 7440-63-3.

## Two-Dimensional NMR Studies of Native Coenzyme F430

Hoshik Won,<sup>†</sup> Karl D. Olson,<sup>‡</sup> Ralph S. Wolfe,<sup>\*,‡</sup> and Michael F. Summers<sup>\*,†</sup>

Contribution from the Department of Chemistry and Biochemistry, University of Maryland Baltimore County, Baltimore, Maryland 21228, and Department of Microbiology, University of Illinois at Urbana-Champaign, Urbana, Illinois 61801. Received August 4, 1989

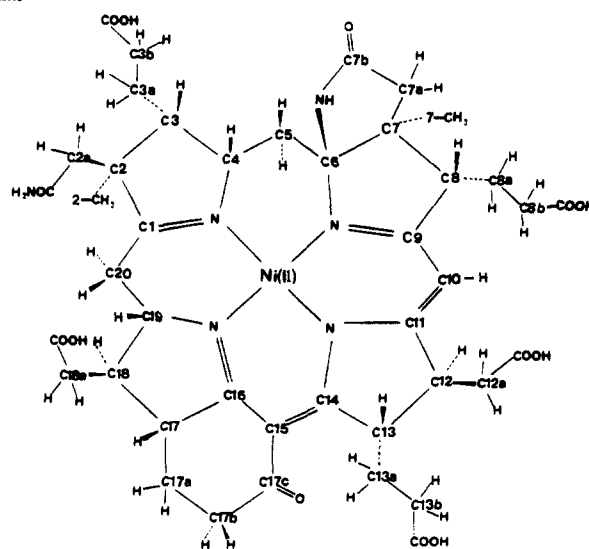
**Abstract:** Modern two-dimensional (2D) NMR spectroscopic methods are used to determine signal assignments and structural features of the recently discovered nickel(II)-containing coenzyme F430. This is the first detailed  $^1\text{H}$  and  $^{13}\text{C}$  NMR study of the native form of coenzyme F430. With the use of COSY, HOHAHA, NOESY, and ROESY  $^1\text{H}$ - $^1\text{H}$  correlated spectroscopies in combination with HMQC and HMBC  $^1\text{H}$ - $^{13}\text{C}$  correlated spectroscopies, signal assignments were made for all carbon atoms and nonexchangeable protons. The data confirm 16 of the 21 specific  $^{13}\text{C}$  NMR signal assignments made earlier for native F430 by classical 1D NMR methods and provide assignment (or reassignment) of the remaining carbon atoms. The  $^1\text{H}$  NMR signal assignments reported here are in good agreement with the partial assignments reported previously for the pentamethyl ester derivative of F430 (F430M) in  $\text{CD}_2\text{Cl}_2$  solution. In addition, long-range through-bond  $^1\text{H}$ - $^{13}\text{C}$  connectivities confirm aspects of the F430 structure deduced from studies of F430M by traditional spectroscopic and chemical methods.

Coenzyme F430, discovered just over 10 years ago, is a nickel-containing cofactor for methyl-coenzyme M reductase that is produced in methanogenic bacteria.<sup>1-4</sup> By an unknown mechanism, F430 mediates the reductive demethylation of methyl-coenzyme M (2-(methylthio)ethanesulfonic acid,  $\text{CH}_3\text{-S-CoM}$ ) using reducing equivalents from (7-mercaptoheptanoyl)threonine phosphate (HS-HTP), producing methane and the heterodisulfide of methyl-coenzyme M and HS-HTP ( $\text{CoM-S-S-HTP}$ ).<sup>5,6</sup> This is the last step in the conversion of  $\text{CO}_2$  to methane in what is believed to be an energy-yielding process in methanogens.

Although single-crystal X-ray data are not available, structural features of F430 have been deduced from extensive chemical and spectroscopic studies of the pentamethyl ester derivative, F430M.<sup>7-10</sup> From several biosynthetically  $^{13}\text{C}$ -labeled F430M samples and with the use of classical one-dimensional (1D) NMR experiments, specific  $^1\text{H}$  and  $^{13}\text{C}$  NMR signal assignments were made for 42 out of 46 total protons and for 21 out of 42 total carbons (excluding methyl ester carbons). Stereochemical assignments were also made for 10 of the 11 chiral corphin ring carbons in F430M. Although studies in aqueous solution were precluded by paramagnetic broadening, a partial  $^{13}\text{C}$  NMR assignment was made for the native (free acid; Chart I) form of F430 in trifluoroethanol (TFE) solution on the basis of comparisons of its 1D  $^{13}\text{C}$  NMR spectrum with the  $^{13}\text{C}$  NMR spectrum obtained for F430M.<sup>9</sup> The  $^1\text{H}$  NMR signals of native F430 in TFE solution were broadened extensively in the 300-MHz spectra and were not assigned or studied in detail.<sup>9</sup>

It has been shown that NMR signal assignments made on the basis of chemical shift analyses and other classical methods are sometimes susceptible to error.<sup>11-13</sup> With the development of new 2D NMR spectroscopic methods that provide long-range

Chart I



through-bond connectivity information, it is possible to determine unambiguously structural elements and NMR signal assignments

- (1) Gunsalus, R. P.; Wolfe, R. S. *FEMS Microbiol. Lett.* **1978**, *3*, 191.
- (2) Diekert, G.; Konheiser, U.; Piechulla, K.; Thauer, R. K. *J. Bacteriol.* **1981**, *148*, 459.
- (3) Walsh, C. T.; Orme-Johnson, W. H. *Biochemistry* **1987**, *26*, 4901.
- (4) Rouviere, P. E.; Wolfe, R. S. *J. Biol. Chem.* **1988**, *263*, 7913.
- (5) Bobik, T. A.; Olson, K. D.; Noll, K. M.; Wolfe, R. S. *Biochem. Biophys. Res. Commun.* **1987**, *149*, 455.
- (6) Ellermann, J.; Hedderich, R.; Boecher, R.; Thauer, R. K. *Eur. J. Biochem.* **1988**, *172*, 669.
- (7) Faessler, A.; Pfaltz, A.; Mueller, P. M.; Farooq, S.; Kratky, C.; Kraeutler, B.; Eschenmoser, A. *Helv. Chim. Acta* **1982**, *65*, 812.

\* To whom correspondence should be addressed.

<sup>†</sup> University of Maryland Baltimore County.

<sup>‡</sup> University of Illinois at Urbana-Champaign.